BioNanoScience (2019) 9:799–812
https://doi.org/10.1007/s12668-019-00670-8

Comparison of Antimicrobial, Antioxidant and Anticancer Activities of ZnO Nanoparticles Prepared by Lemon Juice and Citric Acid Fueled Solution Combustion Synthesis

Prashanth G. K[1,2] · Prashanth P. A[2,3] · Meghana Ramani[4] · Ananda S[5] · Nagabhushana B. M[6] · Krishnaiah G. M[1] · Nagendra H. G[7] · Sathyananda H. M[1] · Mutthuraju M[1] · Rajendra Singh C[7]

Published online: 17 August 2019

Abstract
In the present work, combustion synthesis of ZnO nanoparticles using lemon juice and citric acid as fuels has been carried out. A comparative analysis of the obtained powders has been conducted to understand the strategic advantages of using lemon juice over citric acid as the combustion fuel for the synthesis of ZnO nanopartilcles. The X-ray diffractograms of both the samples revealed the presence of wurtzite hexagonal structure with the standard JCPDS pattern of zincite [36-1451] with varying crystallite sizes. Surface morphology of the samples was studied by scanning electron microscopy. Particle shapes and sizes were determined by transmission electron microscopy. Although wurtzite hexagonal structures were seen in both the synthesis methods, their morphology and sizes differed significantly with samples prepared by lemon juice presenting smaller size. The band gap energy value determined by Wood-Tauc method was found to be ~ 3.2 eV for both the samples. DPPH assay revealed the antioxidant activity of the samples at varied concentrations. Further, antimicrobial studies were greater for those prepared by lemon juice. Furthermore, trypan blue and MTT assay evaluation of nanoparticles against PC-3, HCT116, A549, and MDA-MB-231 cancer cell lines indicated enhanced anticancer activity of ZnO nanoparticles prepared by lemon juice. It was found that the sample prepared using lemon juice exhibited IC_{50} values of 78.80 μg/mL, 28.75 μg/mL, and 10.7 μg/mL, whereas the sample prepared using citric acid as fuel exhibited IC_{50} values of 103.6 μg/mL, 41.52 μg/mL, and 20.06 μg/mL, towards PC-3, HCT 116, and MDA-MB-231 respectively.

Keywords Combustion synthesis · Bio-fuel · Antimicrobial · Antioxidant · Cytotoxicity

✉ Prashanth P. A
prsnthmysore@gmail.com

[1] Department of Chemistry, Sir M. Visvesvaraya Institute of Technology, Bengaluru 562 157, India

[2] Research and Development Centre, Bharathiar University, Coimbatore 641 046, India

[3] Department of Chemistry, P.E.S College of Engineering, Mandya 571 401, India

[4] Center for Nano Science and Nano Technology, Department of Physics and Nano Technology, SRM University, Chennai 603 203, India

[5] Department of Chemistry, University of Mysore, Mysuru 570 006, India

[6] Department of Chemistry, M. S. Ramaiah Institute of Technology, Bengaluru 560 054, India

[7] Department of Bio Technology, Sir M. Visvesvaraya Institute of Technology, Bengaluru 562 157, India

1 Introduction

Nature has elegant and ingenious ways of creating the most efficient miniaturized functional materials. An increasing awareness towards green chemistry and use of green route for synthesis of metal nanoparticles (NPs) lead a desire to develop environment-friendly techniques. Self-propagating high temperature solution combustion synthesis (SCS) is a simple yet reliable technique for the preparation of NPs. Conventionally, organic compounds such as citric acid, urea, and glycine have been used as fuels for the preparation of NPs [1–4]. Recently, the use of naturally available organic materials as fuels has seen upswing owing to the innovative, cheaper, and environmentally neutral implications as opposed to their conventional (chemical) counterparts. Furthermore, naturally extracted entities serve as both reducing and stabilizing agents during the synthesis of NPs [5]. The use of environmentally benign materials, namely, plant extracts,

microorganisms, and enzymes for the synthesis of NPs, offers plentiful benefits such as eco friendliness, biocompatibility, non-toxicity, and cost effectiveness [6–9]. In the present scenario, plants provide a better platform for NPs synthesis as they are non-toxic chemicals [10]. The use of plants as the production assembly of NPs has drawn attention because of its rapid, eco-friendly, economical protocol, providing a single step technique for the biosynthetic processes. Among various plant extracts, phytochemicals are emerging as a useful natural resource for the synthesis of metal/metal oxide NPs. Although phytochemicals are considered non-nutritive, their role as reducing and the stabilizing agents for the synthesis of metal/metal oxide NPs has seen an upsurge in the past decade [11].

ZnO is considered a magic material owing to a plethora of applications: flexibility in preparation, manifestation of various morphologies, and associated properties. Furthermore, ZnO NPs have shown wide variety of applications in the field of textiles [12], catalysis [13], solar cells [14, 15], nano generators [16], food packaging materials [17], gas sensors [18], cosmetics [19], antimicrobials [20], drug delivery [21], cancer therapy [22], etc. Anti diabetic and anti-tubercular activities of ZnO NPs have also been reported recently [23, 24]. Previously, many studies have reported the synthesis of ZnO NPs by conventional fuels such as oxalyl dihydrazide [25], sucrose [26], polyethylene glycol [27], citric acid, glycine, and urea [28]. Also, many studies have reported the use of plant extracts as fuels, such as *Garcinia xanthochymus* [29], *Punica granatum* and *Tamarindus indica* [30], *Cassia fistula* [31], lemon juice [24, 32], *Prunus japonica* [33], *Couroupita guianensis* [34], *Borago officinalis* [35], *Ziziphus nummularia* [36], *Abutilon indicum*, *Melia azedarach*, and *Indigofera tinctoria* [37], in the preparation of metal oxide nanoparrticles by SCS. In our previous work, we have shown the higher anticancer activity of ZnO NPs prepared using bio-fuels as reducing agents over ZnO NPs prepared using a chemical as a reducing agent [37].

Hence, with the above background, in the present work, the potential of lemon juice (over its conventional chemical reagent) as a fuel for the preparation of ZnO NPs using SCS method has been discussed. In this context, our current study emphasizes on the preparation, material characterization, and further antimicrobial, antioxidant, and anticancer activity of ZnO NPs prepared by lemon juice bio-fueled SCS. Samples prepared using both fuels have been compared extensively for their structural, morphological, antimicrobial, antioxidant, and anticancer activities. The objective of this study was to move away from citric acid–based synthesis to a more natural/green synthesis method while comparing the preparation methodology and biological properties of thus synthesized particles with the former.

2 Experimental

2.1 Materials

Zinc nitrate hexahydrate [$Zn(NO_3)_2{\cdot}6H_2O$, AR 99% SD Fine], citric acid [$C_6H_8O_7$, AR 99% SD Fine], potato dextrose agar [3.9% w/v aqueous solution, Himedia], nutrient agar [2.8% w/v aqueous solution, Himedia], Dulbecco's Modified Eagle's medium [DMEM-High Glucose-Himedia], 3-[4, 5-dimethylthiazol-2-yl]-2,5-diphenyl tetrazolium bromide [MTT, $C_{18}H_{16}BrN_5S$, 97.5%, Sigma Aldrich], dimethyl sulfoxide [DMSO, C_2H_6SO, AR 99% Merck], 2,2-diphenyl-1-picrylhydrazyl hydrate [DPPH, $C_{18}H_{12}N_5O_6$, > 90% Merck], ascorbic acid [$C_6H_8O_6$, 98% Sigma Aldrich], fetal bovine serum [FBS, Himedia], (3Z,3′Z)-3,3′-[(3,3′-dimethylbiphenyl-4,4′-diyl) di (1Z) hydrazin-2-yl-1-ylidene] bis (5-amino-4-oxo-3,4-dihydronaphthalene-2,7-disulfonic acid) [Trypan blue, 0.4–0.5% dye concentration, Himedia], phosphate-buffered saline [PBS, 0.86% w/v aqueous solution, Himedia], Amphotericin B [$C_{47}H_{73}NO_{17}$, ~80% Sigma Aldrich], and Ofloxacin [$C_{18}H_{20}FN_3O_4$, ≥98% Sigma Aldrich] were used as such without further purification and fresh lemons from the local market were purchased off the shelf.

2.2 Synthesis of ZnO NPs

ZnO NPs were prepared by SCS as explained in our recent work [24]. The synthesis involves the combustion of redox mixture in which [$Zn(NO_3)_2{\cdot}6H_2O$] acts as an oxidizing agent and lemon juice acts as a reducing agent. 4.0 g of $Zn(NO_3)_2{\cdot}6H_2O$ was dissolved in 40 mL of double-distilled water in a crystalline dish. 9.0 mL of raw lemon juice (filtered) was added to it. The crystalline dish containing the homogeneous mixture was placed in a preheated muffle furnace (375 ± 10 °C). The solution initially underwent dehydration and the resulted viscous liquid caught fire, auto ignited with flames on the surface, which rapidly proceeded throughout the entire volume forming a white powdered product. The sample was calcined at 600 °C for 3 h. The synthesized ZnO was labeled as ZnO (LJ).

Similar method was followed using citric acid (1.57 g) as fuel. The stoichiometry of the redox mixture for combustion was calculated based on the total oxidizing and reducing valencies of the oxidizer and the fuel using the concept of propellant chemistry [2]. The amounts of metal nitrates to fuel ratios for the synthesis of the nanoparticles are based on the following equation:

$$\text{Oxidizer/fuel ratio} = \frac{\sum \text{Valencies of all oxidizing and reducing elements in oxidizer}}{(-1)\ \text{Valencies of all oxidizing and reducing elements in fuel}}$$

ZnO thus synthesized was labeled as ZnO (CA). Both the above reactions yielded white and porous powders within 5–10 min.

2.3 Characterization Techniques

In order to identify the phase purity and crystalline structure of synthesized ZnO NPs, the XRD patterns were recorded with a powder X-ray diffractometer (X'PERT-PRO, Cu-Kα radiation, $\lambda = 1.54$ Å). The formation of ZnO and the absence of any other functional groups from the precursors were confirmed using Fourier-transform infrared spectroscopy (FTIR) by KBr disc method using IRAffinity-1 Shimadzu within the range of 400–3500 cm^{-1}. The UV-Vis absorption spectrum was recorded on JASCO (V-670) at room temperature. The data were analyzed using Origin 8.1 software (Origin Lab Corporation, USA). Morphology of the samples was investigated by Ultra 55, Carl Zeiss, GmbH, field emission scanning electron microscopy (FE-SEM). The shapes and particle size were investigated by high-resolution transmission electron microscopy (HRTEM) carried out on JEOL 3010 instrument with a UHR pole piece. Brunauer-Emmett-Teller (BET) surface area measurements were carried out on Micromeritics ASAP 2020. Average diameter was measured on Brookhaven ZetaPALS. To understand which components of lemon juice are responsible for combustion, a detailed qualitative phytochemical examination was carried out for lemon juice as per the standard methods [38–40]. Estimation of citric acid in lemon juice was carried out by acetic anhydride-pyridine method [41]. In brief, different quantities of citric acid standards (25 to 200 μg) were prepared in clean test tubes and made up the volume into 1 mL with double-distilled water. Eight milliliters of acetic anhydride was added into each test tube and kept in water bath for 10 min at 60 °C. After that, 1 mL of pyridine was added, and allowed to remain in water bath for 40 min at 60 °C. The reaction of acetic anhydride and pyridine gave yellow color to the solution. Following this, they were transferred to an ice-water bath for 5 min. Finally, they were wiped dry and the color intensity was recorded at 420 nm. Fresh lemon juice was centrifuged. One hundred microliters supernatant (filtrate) was taken in a clean test tube and made up the volume to 1 mL with double-distilled water. Eight milliliters of acetic anhydride was added to it and kept in water bath for 10 min at 60 °C. After that, 1 mL of pyridine was added, and again kept in water bath for 40 min at 60 °C. The blank was also maintained containing 1 mL double-distilled water, 8 mL acetic anhydride, and 1 mL pyridine. Citric acid standard was plotted on ordinate and the OD values were plotted on abscissa to determine the concentration of citric acid in lemon juice.

2.4 Evaluation of Antimicrobial Activity by Well Diffusion Method

The antifungal activity of ZnO NPs was carried out by well diffusion method in potato dextrose agar (PDA) media. Petri plates containing 20 mL PDA were seeded with 48–72 h culture of fungal strains *Candida albicans* (*C. albicans*) and *Fusarium oxysporum* (*F. oxysporum*) (10^7 cells/mL, OD 660 nm). Homogeneous dispersions of NPs with different concentrations ranging from 500 to 62.5 μg/mL were prepared by ultrasonication. Wells were cut and the dispersions of ZnO NPs were loaded. The plates were then incubated at 22 °C for 48 h.

The antibacterial activity of ZnO NPs was carried out by well diffusion method in nutrient agar media as explained in our recent report [42]. In brief, 20 mL of sterilized, molten, and cooled nutrient agar media was poured in the sterilized petri dishes. The bacteria *Clostridium perfringens* (*C. perfringens*) and *Salmonella enterica* (*S. enterica*) were cultured overnight at 37 °C in nutrient agar and adjusted to a final density of 10^7 CFU/mL by 0.5 McFarland standards. One hundred microliters of the pathogenic bacteria cultures was transferred onto plate and made culture lawn by using sterile L-rod spreader. Wells were cut and dispersions of ZnO NPs (of different concentrations) were loaded. The plates were then incubated at 37 °C for 24 h. The antimicrobial activity was determined by measuring the diameter of the zone of inhibition (ZOI) formed around the wells. Amphotericin B and Ofloxacin were used as positive controls in antifungal and antibacterial studies respectively.

2.5 Assessment of Antioxidant Activity by DPPH Assay

DPPH radical has a deep-violet color in solution and gradually becomes colorless or pale yellow in the presence of ZnO NPs. This property allows visual monitoring of the reaction and the concentration of radicals is monitored from the change in percentage of absorption [43]. The antioxidant activity of ZnO NPs was measured by DPPH method as reported in the literature with certain modifications [44–53]. A 0.1 mM solution of DPPH in methanol was prepared. One milliliters of this solution was added to 3 mL of the ZnO NPs solution in methanol at different concentrations of 1.0, 0.5, and 0.25 mg/mL. The mixture was shaken vigorously and allowed to stand at room temperature for 30 min in the dark. Absorbance was measured after 30 min at 517 nm using a spectrophotometer. A control reaction was carried out without the test sample. Decrease in the absorbance of DPPH solution indicates an increase in DPPH radical scavenging activity. The percentage of the radical scavenging activity of DPPH was calculated using the following equation:

Percentage of radical scavenging activity = $[(A_c - A_s)/A_c] \times 100$, where A_c and A_s are the absorbance of control and sample respectively. Ascorbic acid was used as the reference standard.

2.6 Determination of Cytotoxicity of ZnO NPs by Trypan Blue Exclusion Assay

To measure the cytotoxicity of the NPs, trypan blue dye was employed to stain the cells that do not have intact membrane. In this test, a cell suspension is simply mixed with dye and then visually examined to determine whether cells take up or exclude dye. In the protocol presented here, a viable cell will have a clear cytoplasm, whereas a nonviable cell will have a blue cytoplasm [54]. Cell suspension of 200 μL was seeded in a 96-well plate at required cell density (20,000 cells/well), without the test agent. The cells were allowed to grow for about 12 h. Dispersions of ZnO NPs of 50 μg/mL and 100 μg/mL were added and the plates were incubated for 24 h at 37 °C in a 5% CO_2 atmosphere. After the incubation period, the plates were taken out from the incubator and the spent media was removed. Twenty microliters of 0.4% trypan blue was added and the images were taken on inverted microscope (Biolink). The tests were carried out in triplicate. The viable cells and dead cells were counted in each image and percentage of viability was calculated as follows:

$$\frac{\text{Total viable cells}}{\text{Totals cell counted}} \times 100$$

2.7 Evaluation of Anticancer Activity by MTT Assay

The cell viability was measured of ZnO NPs by MTT assay as reported in our previous studies [55, 56]. PC-3 is a human prostate cancer cell line, HCT116 is a human colon cancer cell line, A549 cells are adenocarcinomic human alveolar basal epithelial cells, and MDA-MB-231 is a human Caucasian breast adenocarcinoma. These cell lines were chosen given their regular use in tumorigenicity studies. Cytotoxicity of the samples was tested on normal cell line 3T3-L1 (obtained from embryo). Briefly, the cells were seeded in a 96-well plate at a density of 20,000 cells/well. The cells grew for 24 h at 37 °C, 5% CO_2 incubator, and were treated with ZnO NPs in Dulbecco's Modified Eagle's Medium without fetal bovine serum at designed doses from 0 to 300 μg/mL with twofold dilution, for 24 h at 37 °C. One hundred microliters of MTT solution was added to each well and incubated for 3–4 h after removing ZnO NPs containing culture media. Finally, all media were removed and 100 μL of DMSO was added to each well to rapidly solubilize formazan and absorbance was measured at 590 nm. MTT assay was carried out in triplicate. The percent of inhibition was calculated as $[100 - (A_s/A_c) \times 100]$ and cell viability was calculated as $[A_s \times 100/A_c]$, where A_s and A_c are the absorbance values of sample and control respectively.

3 Results and Discussions

3.1 Analysis of Lemon Juice

The results of qualitative phytochemical analysis of lemon juice are summarized in Table 1. The phytochemical results indicate the presence of alkaloids, carbohydrates, reducing sugars, flavanoids, tannins and phenolic compounds, proteins and amino acids, triterpenoids, steroids, and carboxylic acids. These results are in good agreement with previous reports [57, 58]. Carbohydrates, reducing sugars, and carboxylic acids which are present in lemon juice might be responsible for the combustion process in SCS.

Citric acid composition in lemon juice by the standard method followed was found to be 40.12 mg/mL. It would be interesting to note that 9 mL of LJ was used in this combustion process which points towards a ball point amount of 360 mg of CA in LJ. However, 1.57 g of purified CA was used in the complimentary process.

3.2 Pricing Advantage of Lemon Juice over Citric Acid

The cost of purified analytical-grade citric acid is close to Rs. 1.5 per gram when bought from a local supplier in India. In contrast, one lemon in the general market vicinity of Bengaluru (Class A city in India) costs Rs.2 per lemon. We have seen that, on an average, 10–15 mL of LJ can be isolated from a single lemon giving an advantage of price favoring lemon juice over citric acid. Bulk citric acid from Alibaba.com is available at $850/metric ton as opposed to Karnataka trading commission price of Rs.10,000/metric ton of lemon. Taking into account that the average lemon weighs 50 g, one would get close to 20,000 lemons per metric ton. Either way, the pricing is way cheaper for lemon juice when compared with citric acid.

3.3 Crystal Structure

The XRD patterns of ZnO (CA) and ZnO (LJ) are presented in Fig. 1a–b respectively. All the diffraction peaks of XRD pattern could be indexed to pure hexagonal wurtzite type of ZnO [with the standard Joint Committee on Powder Diffraction Standards (JCPDS) No. 36-1451]. As no diffraction peaks were observed from other impurities in the XRD pattern, it was confirmed that pure hexagonal phase ZnO NPs were synthesized through this fast and simple SCS method. The crystallite size is calculated from the full width at half maximum (FWHM) of the diffraction peaks using Scherer's method using the following equation:

$d = k\lambda/\beta \operatorname{Cos} \theta$ where "d" is the average crystalline dimension perpendicular to the reflecting phases, λ is the X-ray wavelength, "k" is Scherer's constant (0.92), β is the full width at half maximum (FWHM) intensity of a Bragg reflection

Table 1 Results of phytochemical screening of lemon juice

Constituent	Test	Result	Constituent	Test	Result
Alkaloids	Mayer's reagent test	+	Tannins and	Lead acetate test	+
	Wagner's reagent test	+	Phenolic	Killer-Killiani test	+
	Hager's reagent test	+	compounds	Ferric chloride test	+
Carbohydrates	Molish's test	+	Saponins	Froth test	−
	Barfoed's test	+	Proteins and	Ninhydrin test	+
Reducing sugars	Fehling's test	+	Amino acids	Biuret test	+
	Benedict's test	+	Triterpenoids	Salwonski test	+
Flavanoids	Alkaline reagent test	+	and	Libermann and	
	Lead acetate test	+	Steroids	Burchard's test	+
Glycoside	Legal's test	–	Carboxylic acids	Sodium bicarbonate test	+
	Bomtrager's test	–		Ester test	+

Note: + indicates presence of phytochemical, - indicates absence of phytochemical

excluding instrumental broadening, and θ is the Bragg's angle. The average crystallite sizes of ZnO (CA), ZnO (LJ) NPs were found to be ~31 and ~26 nm respectively which shows that fuel plays a vital role in the reduction of crystallite size.

3.4 FTIR Analysis

FTIR spectra of ZnO (CA) and ZnO (LJ) NPs are shown in Fig. 1c–d respectively. The peak located at 460–560 cm^{-1} is correlated to the stretching mode of ZnO [59]. The transmittance bands at 1400–1515 cm^{-1} were likely related to absorption of atmospheric CO_2 on the metallic cations; 3450 cm^{-1} indicates the presence of hydroxyl group of water adsorbed on the surface of ZnO NPs [60, 61]. No additional peaks were observed indicating complete reduction.

3.5 Evaluation of Band Gap Energy

A plot of $(\alpha Eg)^{1/2}$ Vs Eg of ZnO (CA) and ZnO (LJ) is shown in Fig. 1e–f respectively. The band gap energy value was determined by Wood-Tauc method [62] as ~3.2 eV for both the samples. This is in good agreement with the literature [63].

3.6 Morphological Studies

The surface morphology of ZnO NPs was studied using SEM. The FE-SEM micrographs of ZnO (CA) and ZnO (LJ) are shown in Fig. 1g–h respectively. These micrographs reveal that besides the spherical crystals, the powders also contain several voids or holes; the reason for which can be attributed to the release of hot gases that escape out of the reaction mixture during combustion [26]. It is through pores of various sizes and shapes that the crystallites are interlinked to one another [26]. SEM micrograph of ZnO (LJ) shows that the particles are highly agglomerated with spongy cave-like structures. It also indicates that sinterable tendency might have increased to form the partially sintered agglomerates. This tendency might be due to increase in surface energy which is the driving force for sintering in combustion process [64].

The HRTEM images of ZnO (CA) and ZnO (LJ) are shown in Fig. 1i–j respectively. Figure 1i shows that the particles are spherical. Figure 1j indicates that the particles are spherical and cubic shaped. The mean particle sizes by histogram were found to be 53 nm and 33 nm for ZnO (CA) and ZnO (LJ) respectively.

3.7 Surface Area Measurements

The surface area of ZnO NPs was measured by the standard BET technique with N_2 adsorption-desorption isotherms on Micromeritics ASAP 2020. The BET surface area values of ZnO (CA) and ZnO (LJ) were found to be 8.191 m^2/g and 10.2373 m^2/g respectively. It was observed that as particle size decreases, the surface area per unit volume or mass increases.

3.8 Particle Size Measurements

Homogeneous dispersions of ZnO NPs were prepared by ultrasonication. Particle size was measured using the dynamic light scattering (DLS) method. The average diameter (mean value of five runs) was found to be 56 nm and 34 nm for ZnO (CA) and ZnO (LJ) respectively. These values are almost similar to the ones calculated from TEM analyses.

Table 2 shows the comparison of particle size measurements by TEM, DLS, and surface area values of ZnO NPs.

3.9 Antimicrobial Activity

The effect of ZnO NPs on different organisms is shown in Fig. 2. The antifungal and antibacterial results on ZnO NPs are presented in Table 3. As observed from the results, the zone of inhibition is maximum at 500 μg/mL indicating that at higher concentrations, the ZnO NPs are exhibiting antimicrobial properties. The results show that the zone of

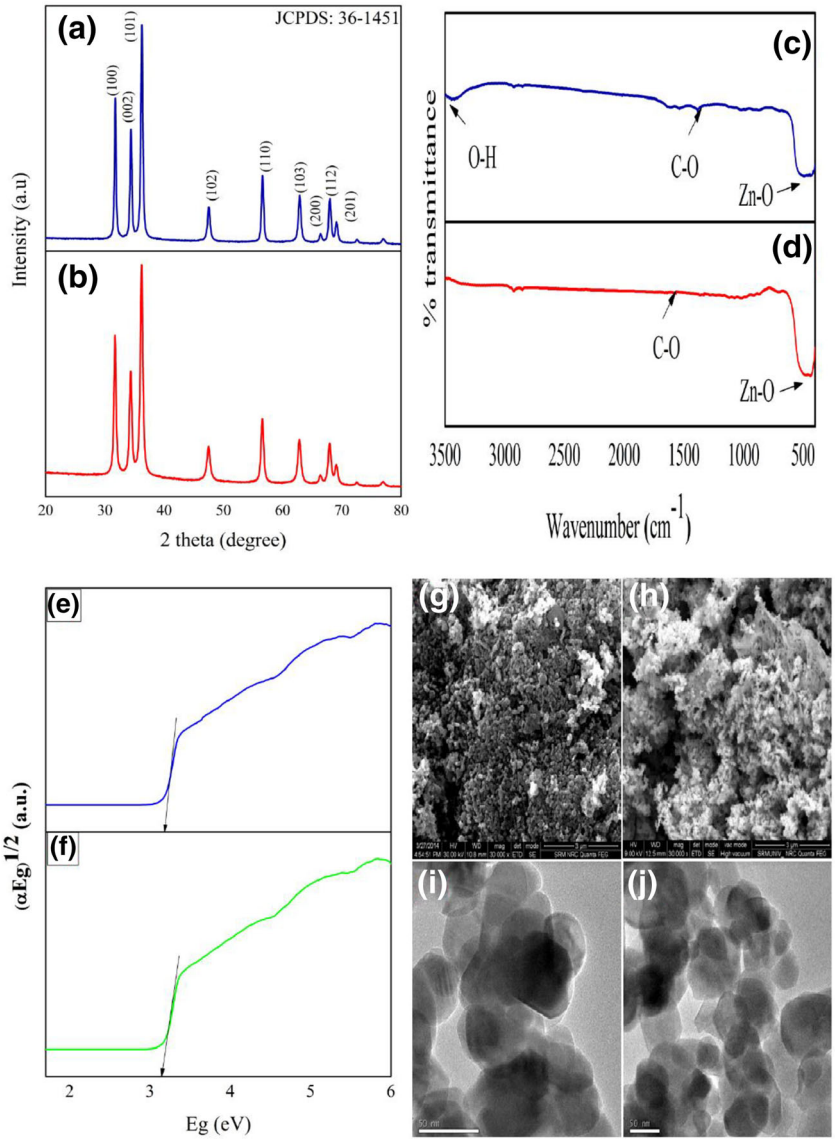

Fig. 1 Powder XRD patterns of (**a**) ZnO (CA) (**b**), ZnO (LJ), FTIR spectra of (**c**) ZnO (CA) (**d**), ZnO (LJ), evaluation of band gap energy of (**e**) ZnO (CA) (**f**), ZnO (LJ), FE-SEM images of (**g**) ZnO (CA) (**h**), ZnO (LJ), HRTEM images of (**i**) ZnO (CA), and (**j**) ZnO (LJ)

inhibition is maximum for ZnO (LJ) against all the organisms than ZnO (CA). Antifungal results indicate that the effect of ZnO NPs is more on *C. albicans* than *F. oxysporum* at all the concentration employed in our studies. Yeasts of *C. albicans* require lower doses of antibiotics and metal NPs such as Ag, Fe_2O_3, and ZnO (6–500 μg/mL), whereas filamentous fungi and the other mold require relatively higher doses (reached 20 mg/mL) of antibiotics and metal NPs. The reason could be attributed as follows: the profuse mycelia mass of the treated molds requires higher dosage for mycelia and spore damage, whereas, the cells of yeast isolates require lower dosage to cause intracellular contents leakage, rupture of cell wall, and finally death of cells leading to loss of microbial cells function [65–68]. As can be visualized from antibacterial results, the zone of inhibition is maximum for ZnO NPs against Gram-positive bacterium *C. perfringens* than the Gram-negative bacterium *S. enteric* as reported previously [69, 70].

The detailed mechanism of the antimicrobial activity of ZnO is still under discussion. Many mechanisms have been proposed related to this: (a) one of the possible mechanisms is based on the abrasive surface texture of ZnO-binding of ZnO NPs to the bacterial surface which is due to electrostatic forces that directly kill bacteria [71], (b) mechanical destruction of the cell membrane caused by penetration of the NPs [72], (c) release of Zn^{2+} ions from the NPs [73], and (d) active oxygen generated from the powder [74–77].

Antimicrobial activity depends on the surface area. This factor has been often claimed relevant [78–82]. In our present studies, ZnO (LJ) showed better antimicrobial activity than ZnO (CA). This might be due to high surface area of ZnO (LJ) than ZnO (CA).

Table 2 Particle size and surface area values of ZnO NPs

Sample by	Mean particle size (nm)		BET surface area
	TEM	by DLS	(m^2/g)
ZnO (LJ)	33	34	10.2373
ZnO (CA)	53	56	8.191

3.10 Antioxidant Activity

The color of DPPH solution gradually changes from deep-violet to pale yellow in the presence of ZnO NPs. The percentage of DPPH scavenging was estimated from the decrease of absorption at 570 nm, which represents the amount of DPPH in the solution. DPPH free radical scavenging activity of ZnO NPs and ascorbic acid with their different concentrations is presented in Fig. 3. The antioxidant activity of ZnO NPs might be due to the transfer of electron density located at oxygen to the odd electron located at nitrogen atom in DPPH resulting the decrease in intensity of $n \rightarrow \pi^*$ transition [43]. These results indicate the higher antioxidant capability of ZnO (LJ) compared with ZnO (CA).

3.11 Trypan Blue Exclusion Assay

In the trypan blue exclusion assay, dead cells with leaky membranes are stained with trypan blue dye, while living cells exclude the blue dye and are not stained. The results showed that the NPs concentration determined the cell survival rate as shown in Fig. 4. Results of cell viability using (a) PC-3, (b) HCT116, (c) A549, and (d) MDA-MB-231 cell lines by trypan blue assay after 24 h of incubation with ZnO NPs are presented in Fig. 5. The results indicate the dissimilar toxicity of ZnO (LJ) and ZnO (CA) on PC-3, HCT116, A549, and MDA-MB-231. Furthermore, the results indicate the higher cytotoxicity of ZnO (LJ) over ZnO (CA) at both the concentrations on all the four cell lines.

3.12 MTT Assay

Cytotoxic effect of ZnO NPs on PC-3, HCT116, A549, MDA-MB-231, and 3T3-L1 cell lines carried out by MTT assay is shown in Fig. 6a–e respectively. Results indicate anti-proliferative response with exposure to ZnO NPs prepared by both lemon juice and citric acid. A typical dose-

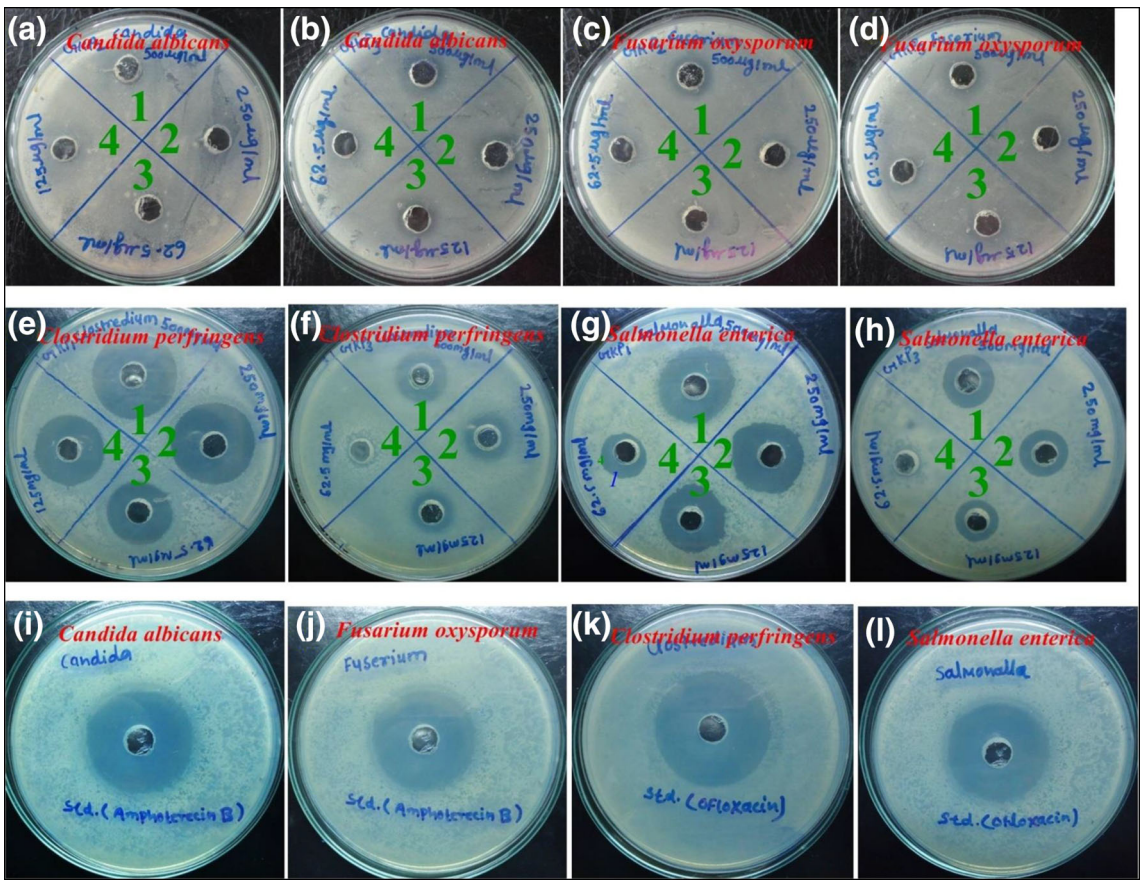

Fig. 2 Zone of inhibition produced by (**a**-**b**) ZnO (LJ) and ZnO (CA) against *C. albicans* respectively (**c**-**d**) ZnO (LJ) and ZnO (CA) against *F. oxysporum* respectively, (**e**-**f**) ZnO (LJ) and ZnO (CA) against *C. perfringens* respectively, (**g**-**h**) ZnO (LJ) and ZnO (CA) against *S. enterica* respectively, (**i**-**l**) standard antibiotic against *C. albicans*, *F. oxysporum*, *C. perfringens*, and *S. enterica* respectively

Table 3 Results of antimicrobial activity of ZnO NPs (zone of inhibition in mm)

Concentration of ZnO suspensions					
Sample	500 μg/mL	250 μg/mL	125 μg/mL	62.5 μg/mL	Positive control 100 μg/mL
ZnO (LJ)	16.00 ± 0.816	13.75 ± 1.50	12.50 ± 1.291	0.00 ± 0.00	*C. albicans*
ZnO (CA)	14.50 ± 1.291	12.00 ± 2.160	9.25 ± 1.258	2.25 ± 4.50	36.25 ± 0.957
ZnO (LJ)	14.75 ± 1.258	12.00 ± 1.414	9.75 ± 0.957	7.25 ± 0.957	*F. oxysporum*
ZnO (CA)	13.50 ± 0.577	11.25 ± 0.957	8.50 ± 0.577	0.00 ± 0.00	36.75 ± 1.258
ZnO (LJ)	34.00 ± 0.816	29.25 ± 0.957	25.50 ± 0.577	21.25 ± 0.957	*C. perfringens*
ZnO (CA)	23.75 ± 0.957	21.25 ± 0.957	17.25 ± 0.957	13.75 ± 0.957	40.75 ± 1.258
ZnO (LJ)	27.25 ± 0.957	24.25 ± 0.957	20.50 ± 1.291	16.75 ± 1.258	*S. enterica*
ZnO (CA)	23.25 ± 1.50	18.75 ± 0.957	15.75 ± 0.957	12.50 ± 1.291	38.00 ± 0.816

Values are the mean ± SE of inhibition zone in mm

dependent response showing increased cell mortality with increase in NPs concentration was clearly observed. Among the four cell lines, both the samples induced dissimilar toxicity with greater toxicity in MDA-MB-231 > PC-3 > A-549 > HCT-116. Previous studies have shown that ZnO NPs illicit different cytotoxic response in a cell-specific and proliferation-dependent manner by rapidly dividing cancer cells being the most susceptible and quiescent cells being the least sensitive [69, 83].

The mechanisms of cytotoxicity from ZnO NPs are not completely understood, but generation of reactive oxygen species (ROS) is believed to be a major component. When NPs interact with cells, cellular defense mechanisms are activated to minimize damage. However, if ROS production exceeds the antioxidative defensive capacity of the cell, it results in oxidative damage of biomolecules which can lead to cell death [84, 85]. ROS is produced inside the cell during various cellular processes, including mitochondrial respiration, inflammatory response, microsome activity, and peroxisome activity [86]. It acts as a biomolecule and plays an important role in cell signaling and homeostasis. Exogenously, ROS is induced in response to various stimuli including nanomaterials [87]. ROS is induced by ZnO NPs in two ways. One is due to the proinflammatory response of the cell against nanoparticles and the other is due to the characteristic surface property of ZnO NPs that makes them a redox reaction system producing ROS [88, 89]. ZnO NPs selectively induce apoptosis in cancer cells, which is likely to be mediated ROS via p53 pathway, through which most of the anticancer drugs trigger apoptosis, where tumor suppressor gene p53 is regarded as the master guardian of the cell and is able to activate cell-cycle checkpoints, DNA repair, and apoptosis to maintain genomic stability [90, 91]. Studies indicate that a primary mechanism of ZnO NPs cytotoxicity might proceed by inducing the generation of ROS, which then are responsible for the induction of apoptosis [69].

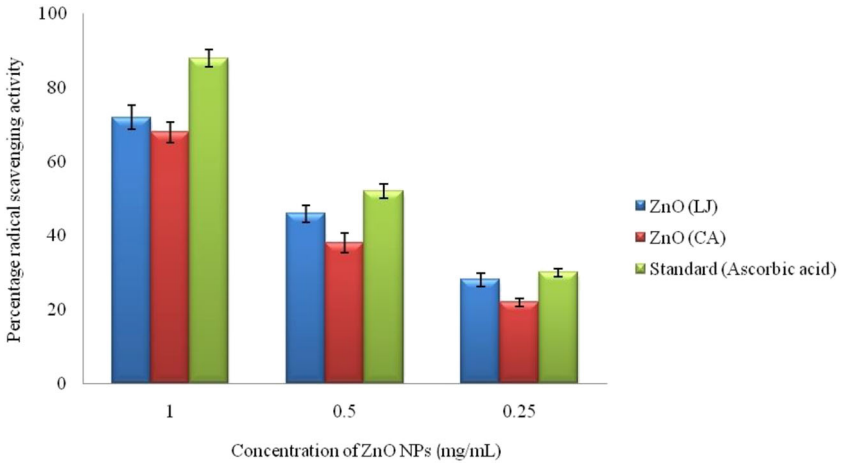

Fig. 3 DPPH free radical scavenging activity of ZnO NPs [data represent mean ± SD (standard deviation)]

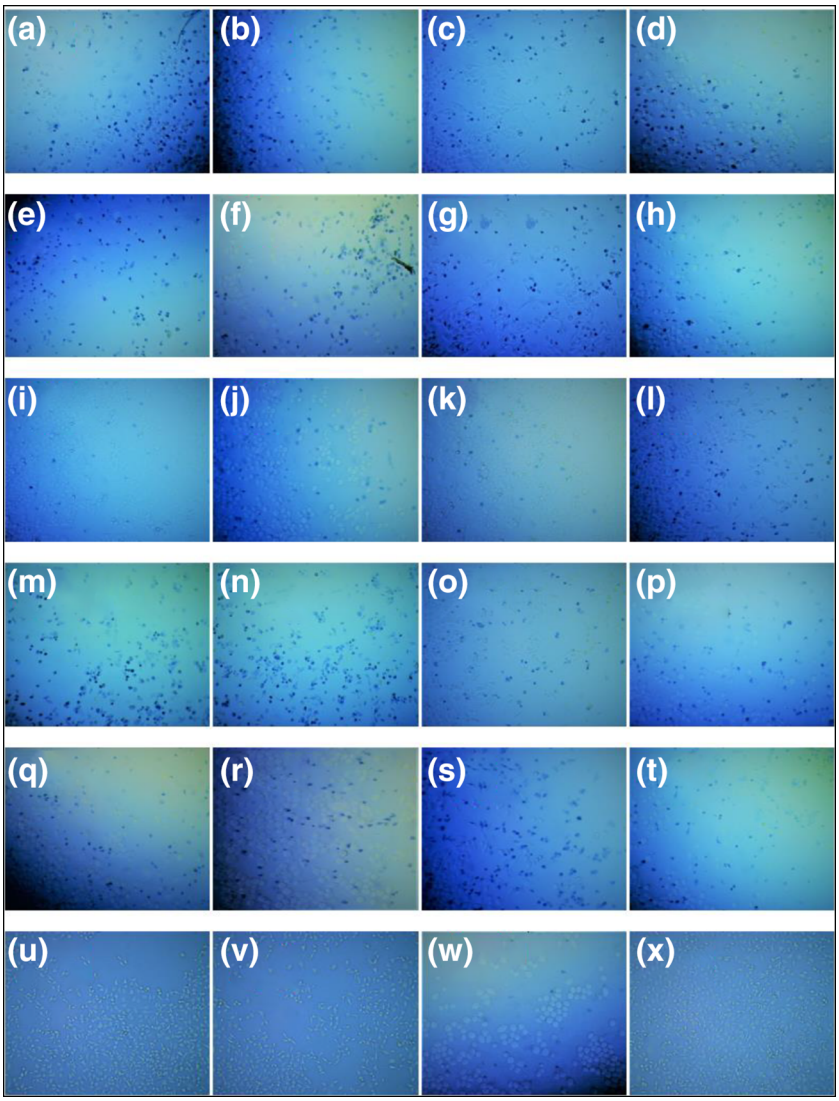

Fig. 4 Cytotoxicity of (**a**-**d**) ZnO (LJ) of 50 μg/mL on PC-3, HCT116, A549, and MDA-MB-231 respectively, (**e**-**h**) ZnO (LJ) of 100 μg/mL on PC-3, HCT116, A549, and MDA-MB-231 respectively, (**i**-**l**) ZnO (CA) of 50 μg/mL on PC-3, HCT116, A549, and MDA-MB-231 respectively, (**m**-**p**) ZnO (CA) of 100 μg/mL on PC-3, HCT116, A549, MDA-MB-231 respectively, (**q**-**t**) positive control Camptothecin (50 μM) on PC-3, HCT116, A549, and MDA-MB-231 respectively, and (**u**-**x**) negative control (medium with cells without ZnO (NPs) on PC-3, HCT116, A549, and MDA-MB-231 respectively after 24 h of incubation at 37 °C using trypan blue exclusion assay. The trypan blue exclusion assay directly determines the cell death. The tests were carried out in triplicate and the data are presented with mean percentage

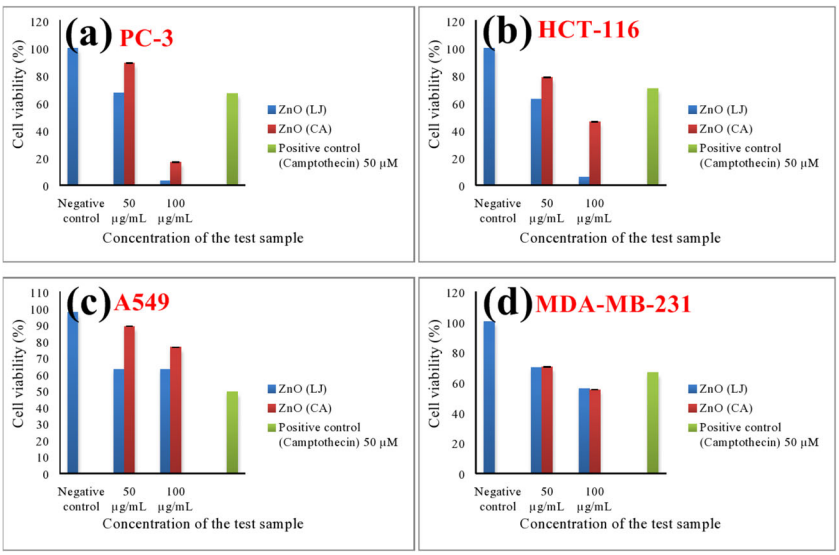

Fig. 5 Results of trypan blue cell viability assay using (**a**) PC-3 (**b**), HCT116 (**c**), A549, and (**d**) MDA-MB-231 cell lines after 24 h of incubation with ZnO NPs

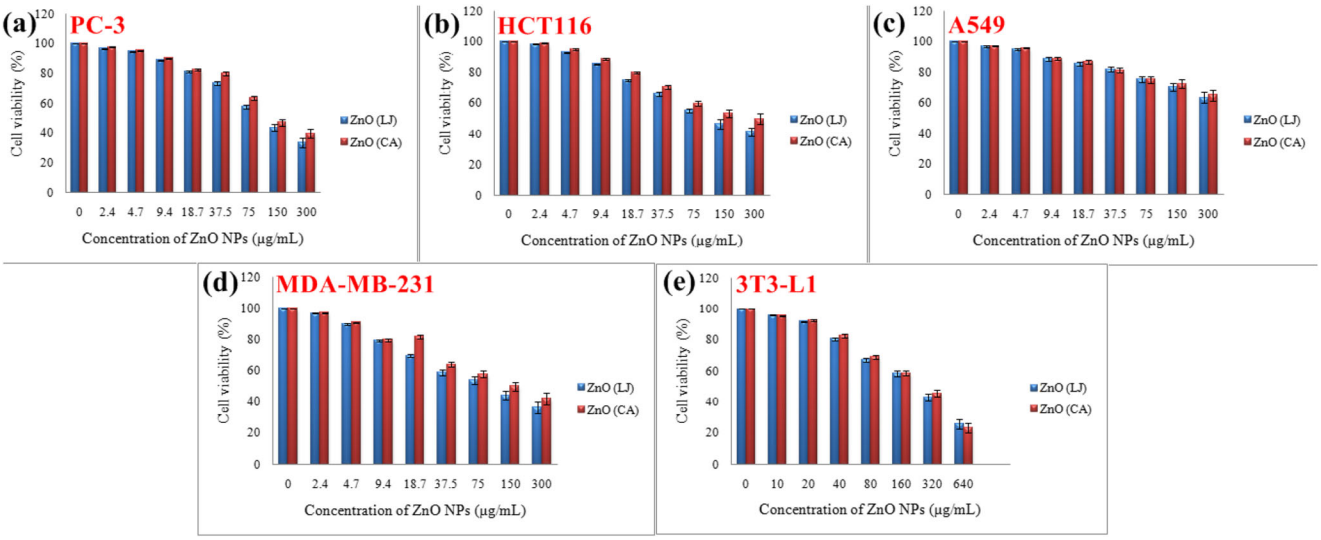

Fig. 6 Cytotoxic effect of ZnO NPs in (**a**) PC-3 (**b**), HCT116 (**c**), A549 (**d**), MDA-MB-231, and (**e**) 3T3-L1 cell lines. Cells were treated with various concentrations of ZnO NPs for 24 h grown in a serum free media. The tests were carried out in triplicate and the percentage of cell death induced was determined using the MTT assay [data represent mean ± SD (standard deviation)]

IC_{50} value, the concentration of ZnO NPs needed to inhibit cell growth by 50% for cytotoxicity test on PC-3, HCT-116, MDA-MB-231, and 3T3-L1 were derived from nonlinear regression analysis (curve fit) based on sigmoid dose response curve (variable) and computed using Graph Pad Prism 5 (Graphpad, San Diego, CA, USA). It is shown in Fig. 7a–d respectively. The IC_{50} values are presented in Table 4 and statistical significance of ZnO (LJ) Vs ZnO (CA) on different cells is shown in Fig. 8. The analysis used was unpaired *t* test with Welch's correction using Graph Pad Prism 5. The MTT test was performed three times which has been used for all the graphs and the standard deviation has been shown in Fig. 8. Though these results confirm that ZnO NPs prepared employing lemon juice as fuel showed slightly better anticancer activity than ZnO NPs prepared using citric acid as fuel, it also indicates that there were no statistically significant results between ZnO (LJ) and ZnO (CA).

Interestingly, IC_{50} values of ZnO (LJ) and ZnO (CA) towards normal cells 3T3-L1 were quite high, i.e., 172.1 µg/mL and 230.6 µg/mL respectively. ZnO NPs exhibited a preferential ability to kill cancerous cells PC-3, HCT-116, and MDA-MB-231 as compared with normal cells 3T3-L1.

Table 4 IC_{50} values (µg/mL) of ZnO NPs in PC-3, MDA-MB-231 cells, and 3T3-L1 after 24 h

Sample	PC-3	HCT116	MDA-MB-231	3T3-L1
ZnO (LJ)	78.80	28.75	10.7	172.1
ZnO (CA)	103.6	41.52	20.06	230.6

Literature survey indicates that ZnO NPs have distinct effects on mammalian cell viability via killing cancer cells (while posing no effect on normal cells) [89]. Earlier studies have shown that ZnO NPs are more toxic to cancer cell and less toxic to normal cells [69, 92–94]. Our results confirm that ZnO NPs showed preferential killing ability to cancer cells PC-3, HCT-116, and MDA-MB-231 compared with non-cancer 3T3-L1 cells. Further, these results with ZnO NPs demonstrate the role of fuels in their synthesis by combustion route and the higher bioactivity of ZnO NPs synthesized using a bio-fuel as reducing agent. As the results of ZnO NPs on MDA-MB-231, HCT-116, and PC-3 are promising, the internal mechanism needs to be discovered in the longer run.

4 Conclusions

The present work was conducted for the evaluation of biological activities of ZnO NPs prepared using two different fuels as reducing agents. Thus prepared NPs were evaluated for their physiochemical, structural, and biological properties and compared with each other to understand the extent of advantage presented by lemon juice over citric acid as a SCS fuel. The samples were characterized by PXRD, FTIR, SEM, HRTEM, DLS, and BET surface area. An estimation of their costs with respect to bench scale and industrial scale production was also done and the results revealed that lemon juice would not only be environmentally benign but also financially advantageous when it comes to large-scale production. Furthermore, it was found that lemon juice contained far lower concentration of citric acid than the quantity used in citric acid synthesis revealing an advantage in terms of

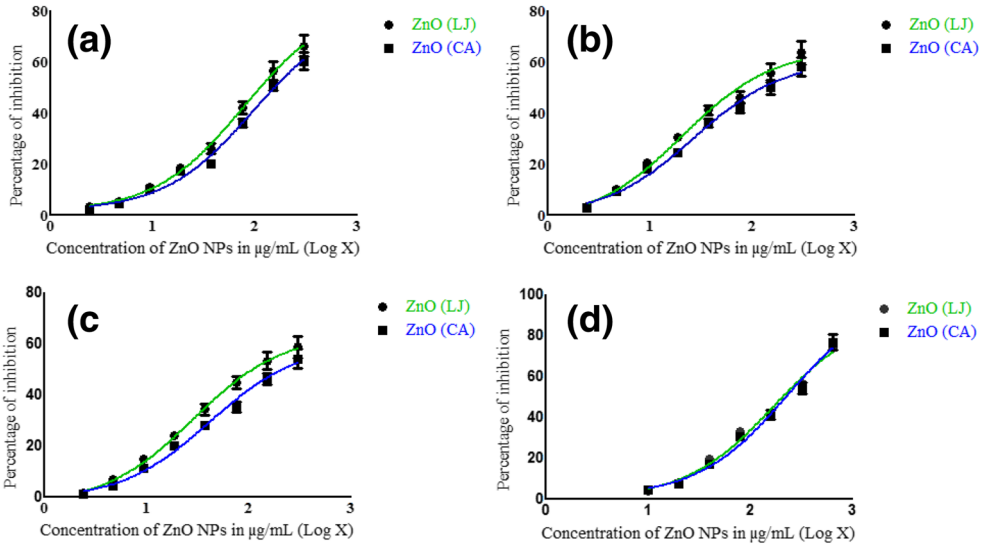

Fig. 7 Determination of IC_{50} (μg/mL) in (**a**) PC-3 (**b**), HCT116 (**c**), MDA-MB-231, and (**d**) 3T3-L1 cell lines [data represent mean ± SD (standard deviation)]

effective volume to active fuel ratio. Both the samples presented hexagonal wurtzite structure with a crystallite size of 25–35 nm. However, it was observed that the sample prepared by lemon juice exhibited lower particle size. Surface area measurements showed higher value of the sample prepared using lemon juice as fuel (10.2373 m^2/g) compared with the sample prepared using citric acid as fuel (8.191 m^2/g). This in-turn showed better bactericidal, antioxidant, and anticancer properties of ZnO NPs prepared by lemon juice. MTT assay and trypan blue assay performed on four cancer cell lines indicated that both the ZnO NPs possess anti-carcinogenic activity. Among the four cell lines, both the samples induced dissimilar toxicity with greater toxicity in MDA-MB-231 > PC-3 > A-549 > HCT-116. Furthermore, it was found that the sample prepared using lemon juice exhibited IC_{50} values of 78.80 μg/mL, 28.75 μg/mL, and 10.7 μg/mL, whereas the sample prepared using citric acid as fuel exhibited IC_{50} values of 103.6 μg/mL, 41.52 μg/mL, and 20.06 μg/mL, towards PC-3, HCT 116, and MDA-MB-231 respectively. Further, sufficiently higher IC_{50} values towards 3T3-L1 (172.1 μg/mL and 230.6 μg/mL) indicate that ZnO NPs are non-toxic for healthy mammalian (mouse) cells. This study concludes with a question that "is lemon juice better than citric acid?" for the synthesis of metal oxide NPs by SCS because, even if the physiochemical, antibacterial, and anticancer properties are better/similar in both cases, we believe that use of lemon juice would be much more cost-effective and less environmentally impactful if this technique is taken to the larger scale. The reason that we think this might be green is because the amount of energy spent on the preparation/purification of citric acid from various sources would not be necessary if lemon juice is used directly.

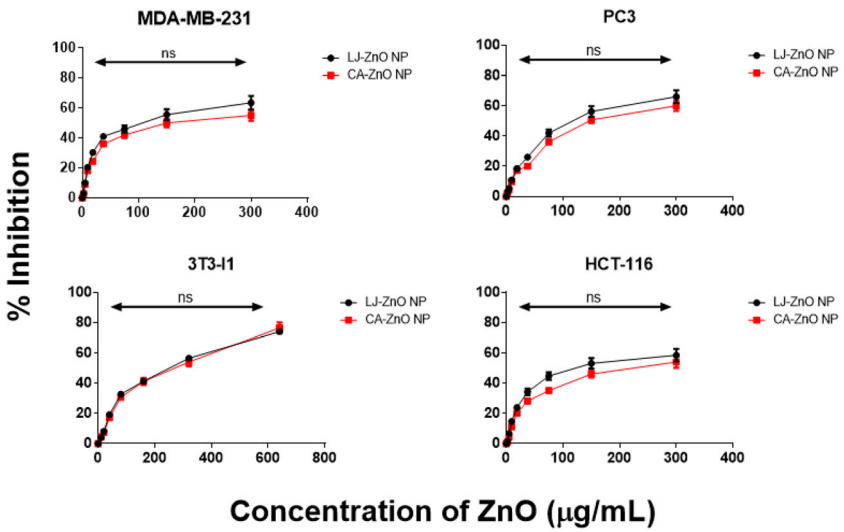

Fig. 8 Statistical significance of ZnO (LJ) Vs ZnO (CA) on PC-3, HCT-116, MDA-MB-231, and 3T3-L1 cell lines. Cells were treated with various concentrations of ZnO NPs for 24 h grown in a serum free media at 37 °C. The percentage of cell death induced was determined using the MTT assay. [The tests were carried out in triplicate and the data represent mean ± SD (standard deviation)]. The analysis used was "Unpaired *t* test with Welch's correction (ns, not-significant)

Acknowledgements The author Prashanth G.K thanks the Management of Sri KET and Principal of Sir MVIT for the support and encouragement extended towards this project. The authors are grateful to Dr. Tejabhiram, Department of Ophthalmology and Visual Sciences, University of Illinois, Chicago for the valuable suggestions. The authors thank Dr. Vivek Polshettiwar, TIFR, Mumbai, for his constant and continued support in BET measurements. The authors acknowledge Nanotechnology Research Center, SRM University, for XRD measurements, IITM for HRTEM analysis, CeNSE, IISc, Bengaluru, for particle size measurements.

Compliance with Ethical Standards

Conflict of Interest None.

Research Involving Humans and Animals Statement Research were conducted "in vitro" without involving humans and animals.

Informed Consent None.

Funding Statement None.

References

1. Patil, K. C., Aruna, S. C., & Mimani, M. (2002). *Current Opinion in Solid State and Materials Science, 6*, 507–512.
2. Patil, K. C., Hegde, M. S., Rattan, T., et al. (2008). *Chemistry of nanocrystalline oxide materials*. Singapore: World Scientific.
3. Nehru, L. C. (2013). Sanjeeviraja C ZnO nanoparticles by citric acid assisted microwave solution combustion method. *Journal of Ceramic Processing Research, 6*, 712–716.
4. Riahi-Noori, N., Sarraf-Mamoory, R., Alizadeh, P., & Mehdikhani, A. (2008). Synthesis of ZnO nano powder by a gel combustion method. *Journal of Ceramic Processing Research, 3*, 246–249.
5. Thakkar, K. N., Mhatre, S. S., & Parikh, R. Y. (2010). Biological synthesis of metallic nanoparticles. *Nanomedicine., 6*, 257–262.
6. Willner, I., Basnar, B., & Willner, B. (2007). Nanoparticle-enzyme hybrid systems for nanobiotechnology. *The FEBS Journal, 274*, 302–309.
7. Mohanpuria, P., Rana, N. K., & Yadav, S. K. (2008). Biosynthesis of nanoparticles: technological concepts and future applications. *Journal of Nanoparticle Research, 10*, 507–517.
8. Verma, V. C., Kharwar, R. N., & Gange, A. C. (2010). Biosynthesis of antimicrobial silver nanoparticles by the endophytic fungus *Aspergillus clavatus*. *Nanomedicine., 5*, 33–40.
9. Saifuddin, N., Wong, C. W., & Yasumira, A. A. N. (2009). Rapid biosynthesis of silver nanoparticles using culture supernatant of bacteria with microwave irradiation. *E-Journal of Chemistry*, 61–70.
10. Prasad, R. (2014). Synthesis of silver nanoparticles in photosynthetic plants. *Journal of Nanoparticles.*
11. Park, Y., Hong, Y. N., Weyers, A., Kim, Y. M., & Linhardt, R. J. (2011). Polysaccharides and phytochemicals: a natural reservoir for the green synthesis of gold and silver nanoparticles. *IET Nanobiotechnology, 3*, 69–78.
12. Abramova, A. V., Abramov, V. O., Gedanken, A., Perelshtein, I., & Bayazitov, V. M. (2014). An ultrasonic technology for production of antibacterial nanomaterials and their coating on textiles. *Beilstein Journal of Nanotechnology, 5*, 532–536.
13. Clament Sagaya Selvam, N., Narayanan, S., John Kennedy, S., & Judith Vijaya, S. (2013). Pure and Mg-doped self-assembled ZnO nano-particles for the enhanced photocatalytic degradation of 4-chlorophenol. *Journal of Environmental Sciences, 25*, 2157–2167.
14. Law, M., Lori, E. G., Justin, C. J., Saykally, R., & Yang, P. (2005). Nanowire dye sensitized solar cells. *Nature Materials, 4*, 455–459.
15. Eita, M., El Labban, A., Cruciani, F., Usman, A., Beaujuge, P. M., & Mohammed OF. (2015). Ambient layer-by-layer ZnO assembly for highly efficient polymer bulk heterojunction solar cells. *Advanced Functional Materials, 25*, 1558–1564.
16. Wang, Z. L., & Song, J. (2006). Piezoelectric nanogenerators based on zinc oxide nanowire arrays. *Science, 312*, 242–246.
17. Espitia, P. J. P., de Fatima Ferreira Soares, N., dos Reis Coimbra, J. S., de Andrade, N. J., Cruz, R. S., & Medeiros, E. A. A. (2012). Zinc oxide nanoparticles: synthesis, antimicrobial activity and food packaging application food safety. *Food and Bioprocess Technology, 5*, 1447–1464.
18. Wan, Q., Li, Q. H., Chen, Y. J., Wang, T. H., He, X. L., Li, J. P., et al. (2014). Fabrication and ethanol sensing characteristics of ZnO nanowire gas sensors. *Applied Physics Letters, 84*, 3654.
19. Lu, P.-J., Huang, S.-C., Chen, Y.-P., Chiueh, L.-C., & Shih, D. Y. C. (2015). Analysis of titanium dioxide and zinc oxide nanoparticles in cosmetics. *Journal of Food and Drug Analysis, 23*, 587–594.
20. Oves, M., Arshad, M., Mohd, S. K., Arham, S. A., Azam, A., & Iqbal, M. I. I. (2015). Targeting water borne bacteria. *Journal of Saudi Chemical Society, 19*, 581–588.
21. Xiong, H.-M. (2013). ZnO nanoparticles applied to bioimaging and drug delivery. *Advanced Materials, 25*, 5329–5335.
22. Sharma, H., Mishra, P. K., Talegaonkar, S., & Vaidya, B. (2015). Metal nanoparticles: theranostic nanotool against cancer. *Drug Discovery Today, 9*, 114–1151.
23. Bayrami, A., Parvinroo, S., Habibi-Yangjeh, A., & Pouran, S. R. (2017). Bio-extract-mediated ZnO nanoparticles: microwave-assisted synthesis, characterization and antidiabetic activity evaluation. *Artificial Cells, Nanomedicine, and Biotechnology*. https://doi.org/10.1080/21691401.2017.1337025.
24. Krishna, P. G., Ananthaswamy, P. P., Trivedi, P., Chaturvedi, V., Mutta, N. B., Sannaiah, A., et al. (2017). Antitubercular activity of ZnO nanoparticles prepared by solution combustion synthesis using lemon juice as bio-fuel. *Materials Science and Engineering: C, 75*, 1026–1033.
25. Prasad, D., Girija, C. R., Jagannatha Reddy, A., Nagabhushana, H., Nagabhushana, B. M., Venkatesha, T. V., & Arun Kumar, S. T. (2014). A study on the antibacterial activity of ZnO nanoparticles prepared by combustion method against *E. coli*. *International Journal of Engineering Research and Applications, 4*, 84–89.
26. Sumana, K. S., Nagabhushana, B. M., Shivakumara, C., Krishna, M., Chandrasekhara Murthy, C. S., & Raghavendra, N. (2012). Photoluminecence studies on ZnO nanopowders synthesized by solution combustion method. *International Journal of Scientific and Research, 1*, 83–86.
27. Inakhunbi Chanu, T., Muthukumar, T., & Manoharan, P. T. (2014). Fuel mediated solution combustion synthesis of ZnO supported gold clusters and nanoparticles and their catalytic activity and in vitro cytotoxicity. *Physical Chemistry Chemical Physics, 16*, 23686–23698.
28. Adriana, C. L., Afonso, R., Paulo, R. C. S., Luiz, F. L., Romulo, A. A., & Luiz, H. D. (2014). ZnO prepared by solution combustion synthesis: characterization and application as photoanode. *Journal of the Brazilian Chemical Society, 25*, 091–1100.
29. Nethravathi, P. C., Shruthi, G. S., Suresh, D., Udayabhanu, N. H., & Sharma, S. C. (2015). Garcinia xanthochymus mediated green synthesis of ZnO nanoparticles: photoluminescence, photocatatlytic and antioxidant studies. *Ceramics International, 41*, 8680–8687.
30. Prashanth, G. K., Prashanth, P. A., Bora, U., Gadewar, M., Nagabhushana, B. M., Ananda, S., Krishnaiah, G. M., & Sathyananda, H. M. (2015). In vitro antibacterial and cytotoxicity studies of ZnO nanopowders prepared by combustion assisted facile green synthesis. *Karbala International Journal of Modern Science, 1*, 67–77.

31. Suresh, D., Nethravathi, P. C., Udayabhanu, R. H., Nagabhushana, H., & Sharma, S. C. (2015). Green synthesis of multifunctional zinc oxide (ZnO) nanoparticles using *Cassia fistula* plant extract and their photodegradative, antioxidant and antibacterial activities. *Materials Science in Semiconductor Processing, 31*, 46–454.
32. Srikanth, C., Chakradhar Sridhar, B., & Mathad, R. D. (2015). Characterization and AC conductivity of novel ZnO doped polyvinyl alcohol (PVA) nano-composite films. *International Journal of Chemical Physical Science, 2*, 78–84.
33. Saravanakumar, A., Peng, M. M., Ganesh, M., Jayaprakash, J., Mohankumar, M., & Jang, H. T. (2016). Low-cost and eco-friendly green synthesis of silver nanoparticles using *Prunus japonica* (Rosaceae) leaf extract and their antibacterial, antioxidant properties. *Artif Cells Nanomed Biotechnol*, 1165–1171.
34. Sathishkumar, G., Logeshwaran, V., Sarathbabu, S., Jha, P. K., Jeyaraj, M., Rajkuberan, C., Senthilkumar, N., & Sivaramakrishnan, S. (2017). Green synthesis of magnetic Fe_3O_4 nanoparticles using *Couroupita guianensis* Aubl. fruit extract for their antibacterial and cytotoxicity activities. *Artificial Cells, Nanomedicine, and Biotechnology*. https://doi.org/10.1080/21691401.2017.1332635.
35. Singh, H., Juan, D., & Tae-Hoo, Y. (2016). Green and rapid synthesis of silver nanoparticles using Borago officinalis leaf extract: anticancer and antibacterial activities. *Artificial Cells, Nanomedicine, and Biotechnology*. https://doi.org/10.1080/21691401.2016.1228663.
36. Padalia, H., & Chanda, S. (2017). Characterization, antifungal and cytotoxic evaluation of green synthesized zinc oxide nanoparticles using ziziphus nummularia leaf extract. *Artificial Cells, Nanomedicine, and Biotechnology*. https://doi.org/10.1080/21691401.2017.1282868.
37. Prashanth, G. K., Prashanth, P. A., Nagabhushana, B. M., Ananda, S., Krishnaiah, G. M., Nagendra, H. G., Sathyananda, H. M., Rajendra Singh, C., Yogisha, S., Anand, S., & Tejabhiram, Y. (2018). Comparison of anticancer activity of biocompatible ZnO nanoparticles prepared by solution combustion synthesis using aqueous leaf extracts of *Abutilon indicum*, *Melia azedarach* and *Indigofera tinctoria* as biofuels. *Artificial Cells, Nanomedicine, and Biotechnology, 46*, 968–979.
38. Farnsworth, N. R. (1966). Biological and phytochemical screening of plants. *Journal of Pharmaceutical Sciences, 55*, 225–276.
39. Harbone, J. B. (1998). *Phytochemical methods* (pp. 60–66). London: Chapman and Hall.
40. Kokate, C. K. (2000). *Practical pharmacognosy* (pp. 107–111). Vallabh Prakashan: Delhi.
41. Odland, R. K. (1971). A study of the acetic anhydride method for the determination of citric acid. Master's Theses p. 796.
42. Krishna, P. G., Ananthaswamy, P. P., Gadewar, M., Bora, U., & Nagabhushna, B. M. (2017). In vitro antibacterial and anticancer studies of ZnO nanoparticles prepared by sugar fueled combustion synthesis. *Advanced Materials Letters, 8*, 24–29.
43. Das, D., Nath, B. C., Phukon, P., Kalita, A., & Dolui, S. K. (2013). Synthesis of ZnO nanoparticles and evaluation of antioxidant and cytotoxic activity. *Colloids and Surfaces. B, Biointerfaces, 111*, 556–560.
44. Khalid, A., Shahid, S., Khan, S. A., Kanwal, S., Yaqoob, A., Rasool, Z. G., & Rizwan, K. (2018). Antioxidant activity and hepatoprotective effect of Cichorium intybus (Kasni) seed extract against carbon tetrachloride-induced liver toxicity in rats. *Tropical Journal of Pharmaceutical Research., 17*(8), 1531–1538.
45. Ashraf, I., Zubair, M., Rizwan, K., Rasool, N., Jamil, M., Khan, S. A., Tareen, R. B., Ahmad, V. U., Mahmood, A., Riaz, M., & Zia-Ul-Haq, M. (2018). Chemical composition, antioxidant and antimicrobial potential of essential oils from different parts of Daphne mucronata Royle. *Chemistry Central Journal., 12*(1), 135.
46. Khan, S. A., Rasool, N., Riaz, M., Nadeem, R., Rashid, U., Rizwan, K., Zubair, M., Bukhari, I. H., & Gulzar, T. (2013). Evaluation of antioxidant and cytotoxicity studies of Clerodendrum inerme. *Asian Journal of Chemistry, 13*, 7457–7462.
47. Khan, S. A., Kanwal, S., Rizwan, K., & Shahid, S. (2018). Enhanced antimicrobial, antioxidant, in vivo antitumor and in vitro anticancer effects against breast cancer cell line by green synthesized un-doped SnO_2 and Co-doped SnO_2 nanoparticles from Clerodendrum inerme. *Microbial Pathogenesis., 125*(C), 366–384.
48. Ahmad, W., Khan, S. A., Munawar, K. S., Khalid, A., & Kawanl, S. (2017). Synthesis, characterization and pharmacological evaluation of mixed ligand-metal complexes containing omeprazole and 8-hydroxyquinoline. *Tropical Journal of Pharmaceutical Research., 16*(5), 1137–1146.
49. Khan, S. A., Noreen, F., Kanwal, S., Iqbal, A., & Hussain, G. (2017). Green synthesis of ZnO and Cu-doped ZnO nanoparticles from leaf extracts of Abutilon indicum, Clerodendrum infortunatum, Clerodendrum inerme and investigation of their biological and photocatalytic activities. *Materials Science and Engineering: C, 82*(C), 46–59.
50. Ijaz, F., Shahid, S., Khan, S. A., Ahmad, W., & Zaman, S. (2017). Green synthesis of copper oxide nanoparticles using Abutilon indicum leaf extract: antimicrobial, antioxidant and photocatalytic dye degradation activities. *Tropical Journal of Pharmaceutical Research., 16*(4), 743–753.
51. Khan, S. A., Ahmad, W., Munawar, K. S., & Kanwal, S. (2018). Synthesis, spectroscopic characterization and biological evaluation of Ni (II), Cu (II) and Zn (II) complexes of diphenyldithiocarbamate. *Indian Journal of Pharmaceutical Sciences., 80*(3), 480–488.
52. Iqbal, A., Khan, Z. A., Shahzad, S. A., Usman, M., Khan, S. A., Fauq, A. H., Bari, A., & Sajid, M. A. (2018). Synthesis of E-stilbene azomethines as potent antimicrobial and antioxidant agents. *Turkish Journal of Chemistry., 42*(6), 1518–1533.
53. Khan, S. A., Noreen, F., Kanwal, S., & Hussain, G. (2017). Comparative synthesis, characterization of Cu-doped ZnO nanoparticles and their antioxidant, antibacterial, antifungal and photocatalytic dye degradation activities. *Digest Journal of Nanomaterials and Biostructures, 12*(3), 877–879.
54. Strober, W. (2001). Trypan blue exclusion test of cell viability. *Current Protocols in Immunology*. https://doi.org/10.1002/0471142735.ima03bs21.
55. Krishna, P. G., Ananthaswamy, P. P., Yadavalli, T., Mutta, N. B., Sannaiah, A., & Shivanna, Y. (2016). ZnO nanopellets have selective anticancer activity. *Materials Science and Engineering: C, 62*, 919–926.
56. Prashanth, G. K., Prashanth, P. A., Nagabhushana, B. M., Ananda, S., Nagendra, H. G., & Rajendra Singh, C. (2016). In vitro antimicrobial, antioxidant and anticancer studies of ZnO nanoparticles synthesized by precipitation method. *Advanced Science, Engineering and Medicine, 8*, 306–313.
57. Bansode, S., & Chavan, M. D. (2012). Studies on antimicrobial activity and phytochemical analysis of citrus fruit juices against selected enteric pathogens. *Internationl Research Journal of Pharmacy, 3*, 122–126.
58. Mathew, B. B., Jatawa, S. K., & Tiwari, A. (2012). Phytochemical analysis of citrus limonum pulp and peel. *International Journal of Pharmacy and Pharmaceutical Sciences, 4*, 269–371.
59. Ismail, H. M. (1991). A thermo analytic study of metal acetylacetonates. *Journal of Analytical and Applied Pyrolysis, 21*, 315–326.
60. Dutta, S., & Bichitra, N. G. (2012). Characterization of ZnO nanoparticles grown in presence of folic acid template. *Journal of Nanobiotechnology, 10*, 29.

61. Kumar, H., & Rani, R. (2013). Structural and optical characterization of ZnO nanoparticles synthesized by microemulsion route. *International Letters of Chemistry, Physics and Astronomy, 14*, 26–36.
62. Tauc, J. (1970). *Optical properties of solids. Ed. F. Abeles*. Amsterdam: North-Holland Publ.
63. Kolekar, T. V., Bandgar, S. S., Shirguppikar, S. S., & Ganachari, V. S. (2013). Synthesis and characterization of ZnO nanoparticles for efficient gas sensors. *Archives of Applied Science Research, 5*, 20–28.
64. Roy, T. K., Bhowmick, D., Sanyal, D., & Chakrabarti, A. (2008). Sintering studies of nano-crystalline zinc oxide. *Ceramics International, 34*, 81–87.
65. Hassan, A. A., Howayda, M. E., & Mahmoud, H. H. (2013). Effect of zinc oxide nanoparticles on the growth of mycotoxigenic mould. *Studies in Chemical Process Technology, 4*, 66–74.
66. Nabway, G. A., Hassan, A. A., & Sayed El-Ahl, R. H. (2014). Effect of metal nanoparticles in comparison with commercial antifungal feed additives on the growth of *Aspergillus flavus* and Aflatoxin B_1 production. *Journal of Biosciences, 3*, 954–971.
67. Hassan, A. A., Noha, H. O., & El-Dahshan, A. M. A. (2015). Antimicrobial potential of iron oxide nanoparticles in control of some causes of microbial skin affection in cattle. *European Journal of Academic Essays, 2*, 20–31.
68. Aliaa, E. M., Atef, A. H., Hassan, M. A., El Hariri, M., & Refai, M. (2015). Effect of metal nanoparticles on the growth of ochratoxigenic moulds and ochratoxin A production isolated from food and feed. *International Journal of Research Studies in Biosciences (IJRSB), 3*, 1–14.
69. Premanathan, M., Karthikeyan, K., Jeyasubramanian, K., & Manivannan, G. (2011). Selective toxicity of ZnO nanoparticles toward Gram-positive bacteria and cancer cells by apoptosis through lipid peroxidation. *Nanomedicine, 7*, 184–192.
70. Azam, A., Ahmed, A. S., Oves, M., Khan, M. S., Habib, S. S., & Memic, A. (2012). Antimicrobial activity of metal oxide nanoparticles against Gram-positive and Gram-negative bacteria: a comparative study. *International Journal of Nanomedicine, 7*, 6003–6009.
71. Stoimenov, P. K., Klinger, R. L., Marchin, G. L., & Klabunde, K. J. (2002). Metal oxide nanoparticles as bactericidal agents. *Langmuir, 18*, 6679–6686.
72. Brayner, R., Ferrari-Iliou, R., Brivois, N., Djediat, S., Benedetti, M. F., & Fievet, F. (2006). Toxicological impact studies based on *Escherichia coli* bacteria in ultrafine ZnO nanoparticles colloidal medium. *Nano Letters, 6*, 866–870.
73. Heinlaan, M., Ivask, A., Blinova, I., Dubourguier, H. C., & Kahru, A. (2008). Toxicity of nanosized and bulk ZnO, CuO and TiO_2 to bacteria *Vibrio fischeri* and crustaceans *Daphnia magna* and *Thamnocephalus platyurus*. *Chemosphere, 71*, 1308–1316.
74. Xu, T., & Xie, C. S. (2003). Tetrapod-like nano-particle ZnO/acrylic resin composite and its multi-function property. *Progress in Organic Coatings, 46*, 297–301.
75. Zhang, L. L., Jiang, Y. H., Ding, Y. L., Povey, M., & York, D. (2007). Investigations into the antibacterial behavior of suspensions of ZnO nanoparticles (ZnO nanofluids). *Journal of Nanoparticles, 9*, 479–489.
76. Franklin, N. M., Rogers, N. J., Apte, S. C., Batley, G. E., Gadd, G. E., & Casey, P. S. (2007). Comparative toxicity of nanoparticulate ZnO, bulk ZnO, and $ZnCl_2$ to a freshwater microalga (Pseudokirchneriella subcapitata): the importance of particle solubility. *Environmental Science & Technology, 41*, 8484–8490.
77. Yang, H., Liu, C., Yang, D., & Xi, Z. (2009). Comparative study of cytotoxicity, oxidative stress and genotoxicity induced by four typical nanomaterials: the role of particle size, shape and composition. *Journal of Applied Toxicology, 29*, 69–78.
78. Akhavan, O., Mehrabian, M., Mirabbaszadeh, K., & Azimirad, R. (2009). Hydrothermal synthesis of ZnO nanorod arrays for photocatalytic inactivation of bacteria. *Journal of Physics D: Applied Physics, 42*.
79. Lipovsky, A., Tzitrinovich, Z., Friedmann, H., Applerot, G., Gedanken, A., & Lubart, R. (2009). EPR study of visible light-induced ROS generation by nanoparticles of ZnO. *The Journal of Physical Chemistry, 113*, 15997–16001.
80. Zhang, L., Ding, Y., Povey, M., & York, D. (2008). ZnO nanofluids - a potential antibacterial agent. *Progress in Natural Science, 18*, 939–944.
81. Amornpitoksuk, A. P., Suwanboon, S., Sangkanu, S., Sukhoom, A., Wudtipan, J., Srijan, K., & Kaewtaro, S. (2011). Synthesis, photocatalytic and antibacterial activities of ZnO particles modified by diblock copolymer. *Powder Technology, 212*, 432–438.
82. Vatsha, B., Tetyana, P. L., Shumbula, P. M., Ngila, J. C., Sikhwivhilu, L. M., & Moutloali, R. M. (2013). Effects of precipitation temperature on nanoparticle surface area and antibacterial behavior of $Mg(OH)_2$ and MgO nanoparticles. *Journal of Biomedical Nanotechnology, 4*, 365–373.
83. Hanley, C., Layne, J., Punnoose, A., Reddy, K. M., Coombs, I., Coombs, A., Feris, K., & Wingett, D. (2008). Preferential killing of cancer cells and activated human T cells using ZnO nanoparticles. *Nanotechnol, 19*, 295103.
84. Carmody, R. J., & Cotter, T. G. (2001). Signaling apoptosis: a radical approach. *Redox Report, 6*, 77–90.
85. Ryter, S. W., Kim, H. P., Hoetzel, A., Park, J. W., Nakahira, K., Wang, X., et al. (2007). Mechanisms of cell death in oxidative stress. *Antioxidants & Redox Signaling, 9*, 49–89.
86. Bisht, G., & Rayamajhi, S. (2016). ZnO nanoparticles: a promising anticancer agent. *Nanobiomedicine, 3*, 9.
87. Manke, A., Wang, L., & Rojanasakul, Y. (2013). Mechanisms of nanoparticle-induced oxidative stress and toxicity. *BioMed Research International*, 15.
88. Rasmussen, J. W., Martinez, E., Louka, P., & Wingett, D. G. (2010). Zinc oxide nanoparticles for selective destruction of tumor cells and potential for drug delivery applications. *Expert Opinion on Drug Delivery, 7*, 1063–1077.
89. Wilson, M. R., Lightbody, J. H., Donaldson, K., Sales, J., & Stone, V. (2002). Interactions between ultrafine particles and transition metals in vivo and in vitro. *Toxicology and Applied Pharmacology, 184*, 172–179.
90. Akhtar, M. J., Ahamed, M., Kumar, S., Majeed Khan, M. A., Ahmad, J., & Alrokayan, S. A. (2012). Zinc oxide nanoparticles selectively induce apoptosis in human cancer cells through reactive oxygen species. *International Journal of Nanomedicine, 7*, 845–857.
91. Sherr, C. J. (2004). Principles of tumor suppression. *Cell, 11*, 235–246.
92. Bakhori, S. K. M., Mahmud, S., Ann, L. C., Mohamed, A. S., Saifuddin, S. N., Masudi, S.'a. M., et al. (2015). Toxicity evaluation of ZnO nanostructures on L929 fibroblast cell line using MTS assay. *AIP Conference Proceedings, 1657*, 040001.
93. Paino, I. M. M., Gonçalves, F. J., Souza, F. L., & Zucolotto, V. (2016). Zinc oxide flower-like nanostructures that exhibit enhanced toxicology effects in cancer cells. *ACS Applied Materials & Interfaces, 8*, 32699–32705.
94. Renschler, M. F. (2004). The emerging role of reactive oxygen species in cancer therapy. *European Journal of Cancer Therapy, 40*, 1934–1940.